# Thermomechanical processing of (TiB + TiC)/Ti matrix composites and effects on microstructure and tensile properties

Changjiang Zhang,[a] Shuzhi Zhang,[b] and Peng Lin
*Shanxi Key Laboratory of Advanced Magnesium-based Materials, Taiyuan University of Technology, Taiyuan 030024, Shanxi, People's Republic of China; and Department of Materials Processing Engineering, School of Materials Science and Engineering, Taiyuan University of Technology, Taiyuan 030024, Shanxi, People's Republic of China*

Zhaoping Hou
*Department of Materials Science, School of Materials Science and Engineering, Taiyuan University of Technology, Taiyuan 030024, Shanxi, People's Republic of China*

Fantao Kong and Yuyong Chen
*National Key Laboratory for Precision Hot Processing of Metals, Harbin Institute of Technology, Harbin 150001, Heilongjiang, People's Republic of China*

(Received 18 October 2015; accepted 22 March 2016)

In the paper, 2.5 vol% (TiB + TiC)/Ti composite has been fabricated by in situ casting route. 1-D forging and subsequent multistep rolling in (α + β) phase field are conducted on the as-cast composite and, accordingly, the matrix microstructure is significantly refined, and the distribution uniformity of reinforcements is greatly improved. The tensile properties of the composites with different processing states are tested at room temperature (RT), 600 and 700 °C. The results indicate that thermomechanical processing (TMP) can drastically improve strength and elongation of the as-cast composite both at RT and 600 °C. As tensile temperature increases to 700 °C, the UTSs of the composites gradually reduce while the elongations of the composites are enhanced remarkably after TMP. The degradation in UTS can be related to the matrix softening and interfacial debonding at 700 °C.

## I. INTRODUCTION

Specific modulus, high strength, superior creep, and fatigue resistances are the salient features that make titanium matrix composites (TMCs) promising for a variety of applications.[1–3] Especially, particulate reinforced TMCs (PRTMCs) prepared by in situ technique have drawn great attention because of the ease of fabrication and low processing cost.[4,5] Among the various reinforcements used in PRTMCs, TiB, and TiC are of particular interest owing to their popular balance of modulus, stability, and similarity of heat expansion coefficients with Ti matrix.[1,6,7] Currently, (TiB + TiC)/Ti composites can be in situ synthesized by many methods, among which combustion assisted cast is more popular due to its obvious technical advantage.[1,8,9]

As is well known, the main drawbacks that restrict the application of as-cast PRTMCs are the low ductility at room temperature (RT) and limited performance at high temperature. Therefore, it is necessary to improve reinforcement distribution and refine matrix microstructure by thermomechanical processing (TMP) so as to improve the mechanical properties of as-cast composites. Recent study by Imayev et al.[10] has shown that the Ti–TiB-based composites exhibit much higher strength than matrix alloy without drastic ductility reduction after multiple isothermal 2-D forging. Rastegari et al.[11] also found that elongation achieves 10% when the as-cast TiC/Ti–6Al–4V composite undergone direct rolling with a total deformation of 40%. It is noted that the hot working of TMCs mostly concentrated in the β phase field while little attention has been paid to the hot working process in (α + β) phase field. Actually, numerous studies[12–14] carried out on titanium alloys have revealed that equiaxed and bimodal microstructures can be obtained by TMP in (α + β) phase field. And the equiaxed microstructure with good plasticity and low cycle fatigue properties while the bimodal microstructure with good fatigue and creep resistant properties are generally recognized.[13,14] Thus, it's essential to systematically research the microstructure and mechanical properties of (TiB + TiC)/Ti composites processed in (α + β) phase field.

In this study, the 2.5 vol% (TiB + TiC)/Ti composite was prepared by in situ casting route then underwent forging and rolling in (α + β) phase field. The main objective of the present work was to investigate the relationship among TMP, microstructural evolution, and tensile properties.

Contributing Editor: Jürgen Eckert
Address all correspondence to these authors.
[a]e-mail: zcj0408@163.com
[b]e-mail: zhshzh1984@163.com
DOI: 10.1557/jmr.2016.143

 © Materials Research Society 2016

https://doi.org/10.1557/jmr.2016.143 Published online by Cambridge University Press

## II. EXPERIMENTAL PROCEDURE

### A. Materials preparation

In this experiment, the material used is Ti–6Al–2.5Sn–4Zr–0.7Mo–0.3Si matrix alloy reinforced with 2.5 vol% (TiB + TiC) (volume fraction ratios, TiB:TiC = 1:1). sponge titanium (99.9%), $B_4C$ powder (98%, average particle size 5–10 μm), graphite powder (99%, average particle size 1–2 μm), and other alloying elements such as Al (99.99%), Sn (99.9%), sponge Zr (99.9%), crystal Si (99.9%), Al–Mo and Al–Y master alloys were chosen as raw materials. Induction skull melting technique was adopted to prepare the composite ingot with a length of 120 mm and a diameter of 140 mm. The specific β-transus temperature of the composite measured through metallographic techniques is approximately 1080 °C.

After casting, the composite ingot underwent one-dimensional forging at 1050 °C with a total deformation of 70% followed by air cooling. Then the as-forged composite was hot rolled at 1000 °C through three passes, with nominal reduction of approximately 40% per pass. The 2.5 vol% (TiB + TiC)/Ti composite sheet was obtained after the last pass of rolling followed by air cooling. Finally, the composite sheet was subjected to heat treatment at 650 °C for 6 h followed by furnace cooling to eliminate the stress during rolling.

### B. Microstructure examination and tensile testing

Samples for microstructural observation and tensile test were cut by electric discharging from the ingot, pancake, and sheet of 2.5 vol (TiB + TiC)/Ti composite. Microstructure observations were examined by FEI-Quanta-200F scanning electron microscope (SEM; FEI Company, Hillsboro, Oregon) and Philips-CM12 transmission electron microscopy (TEM; FEI Company, Eindhoven, The Netherlands). To investigate the characteristic of reinforcements and the matrix microstructure, the image analysis software Image-Pro Plus was used to analyze the SEM images. Tensile tests were carried out on an INSTRON-5500R testing machine (Instron, Norwood, Massachusetts) at a constant crosshead speed of 0.5 mm/min at RT and elevated temperature. The gauge sections of the RT and elevated temperature tensile specimens are 20 mm × 6 mm × 2 mm and 20 mm × 5 mm × 2 mm, respectively. Three samples for tensile tests were carried out at each condition to ensure repeatability. And Hitachi S-570 SEM (Hitachi Limited, Tokyo, Japan) was adopted to observe the fracture surfaces after tensile tests.

## III. RESULTS AND DISCUSSION

### A. Microstructure

Figure 1 presents the microstructure of the as-cast composite. α–β two-phase matrix microstructure and reinforcements mainly located at the prior β grain boundaries can be obviously observed in Fig. 1(a). The measured average α lath width and prior β grain size are 6.82 and 137.9 μm, respectively. The prior β grain size is apparently smaller than that of the as-cast matrix alloy [about 1033.2 μm (Ref. 15)]. Similar grain refinement effects are also found in other boron or carbon containing titanium alloys,[16–18] indicating the significant refinement effect of B and C elements. As B and C elements are almost insoluble in titanium, the enrichment of B and C elements at the front of liquid/solid interface during solidification causes constitutional undercooling, hence the nucleation rate increases and grains are refined.[16,17,19] The reinforcements segregated at the prior grain boundaries exhibit two different morphologies, i.e., short-fiber shape of TiB and near-equiaxed shape of TiC [as indicated by the arrows in Fig. 1(b)] distinguished by spectrum analysis techniques. The different morphologies of TiB and TiC reinforcements can be related to their different crystal structures and solidification paths.[2] The aspect ratio of TiB whiskers and TiC particles was measured by image analysis software, which is 8.56

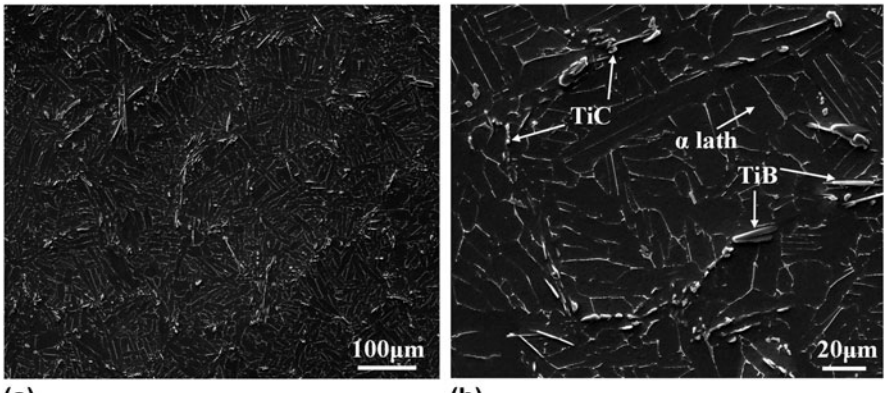



FIG. 1. Microstructure of the as-cast composite showing: (a) distribution of reinforcement and (b) matrix within the composite.



https://doi.org/10.1557/jmr.2016.143 Published online by Cambridge University Press

and 2.49, respectively. As known, good interface bonding between the reinforcements and matrix can contribute to strengthening the TMCs. Fortunately, previous study[15] on interfaces by TEM has revealed that the interfaces are clean, thereby promoting the strong bonding between matrix and reinforcements.

Figure 2 shows the microstructure of the composite forged at 1050 °C with a reduction of approximatively 70%. As shown in Fig. 2(a), TiB and TiC reinforcements distributed at prior β grain boundaries (Fig. 1) are rotated and slightly oriented perpendicular to forging direction. However, the segregation of TiB and TiC reinforcements

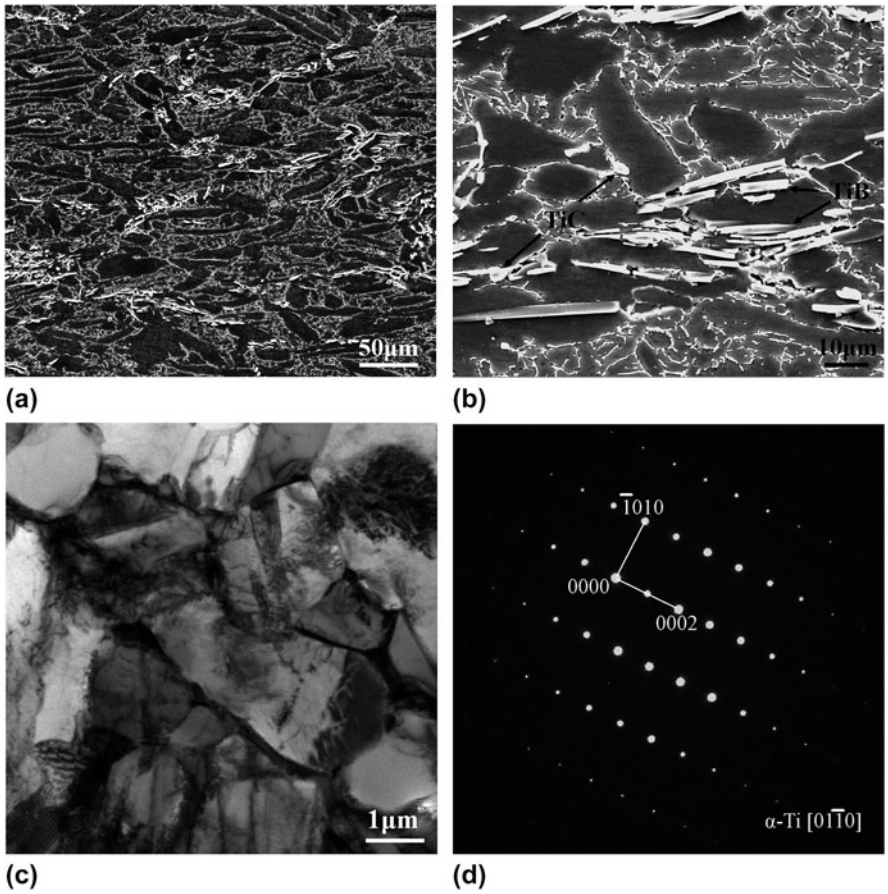



FIG. 2. The microstructure of the as-forged composite: (a) SEM image, (b) magnified SEM image, (c) bright-field TEM image, and (d) selected area electron diffraction (SAED) pattern of α-Ti phase shown in (c).

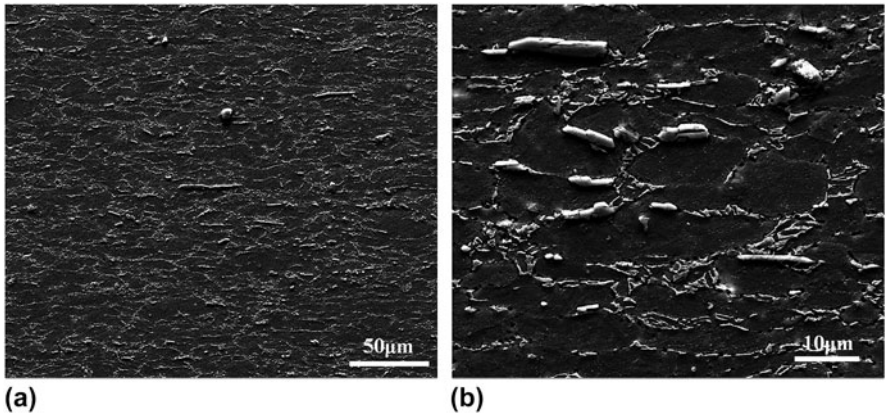



FIG. 3. SEM images showing microstructures of the as-rolled composite sheet: (a) distribution of TiB whiskers and (b) matrix within the composite.

https://doi.org/10.1557/jmr.2016.143 Published online by Cambridge University Press

can be still observed though the distribution uniformity of the reinforcements is considerably enhanced due to reduction in aspect ratio of reinforcements after 1-D forging (the aspect ratio of TiB and TiC are 5.28 and 1.96, severally). In addition, it is noted that microvoids can be found at the ends of TiB whiskers and the edges of TiC particles in high magnification micrograph shown in Fig. 2(b). Analogously, because of the lower thermomechanical processing temperature[20] and unoptimized processing parameters,[21] microvoids left after reinforcement fracture are observed. Thus, the insufficient matrix flow is unable to well fill the resulting microvoids caused by the mismatched deformation between reinforcement and matrix.

For the matrix microstructure of the as-forged composite, the bimodal microstructure consisting of equiaxed primary α phase ($\alpha_p$) and a transformed β phase matrix can be observed in Figs. 2(a) and 2(b), which are due to the deformation in the two α + β phase field followed by air cooling. The volume fraction and aspect ratio of the $\alpha_p$ are measured to be 42.6% and 2.28, respectively. It is noted that the current secondary α is near-equiaxed morphology with an average size of about 3.7 μm. And the morphology is different from the common secondary α within transformed β phase matrix, which is lamellar structure after thermomechanical processing in (α + β) phase field.[21] The result can be related to the precipitation mechanism of secondary α during cooling process after forging. Normally, the secondary α nucleates on β phase and grows rapidly during the solid state transformation (β → β + α) after high cooling rate. However, the secondary α can also nucleate on the $\alpha_p$ and grow slowly under low cooling rate.[22] Moreover, the presence of TiB and TiC reinforcements can provide additional nucleation sites for the secondary α as well. Thus, the secondary α does not exhibit lamellar shape but near-equiaxed morphology under the aforesaid influencing factors. Through TEM micrograph shown in Fig. 2(c) substructures in α phase can be observed in the forged composite. It can be seen the α subgrains are very fine with an average size of about 1.3 μm. Based on the previous studies,[22,23] the TiB and TiC reinforcements can impede the movement of

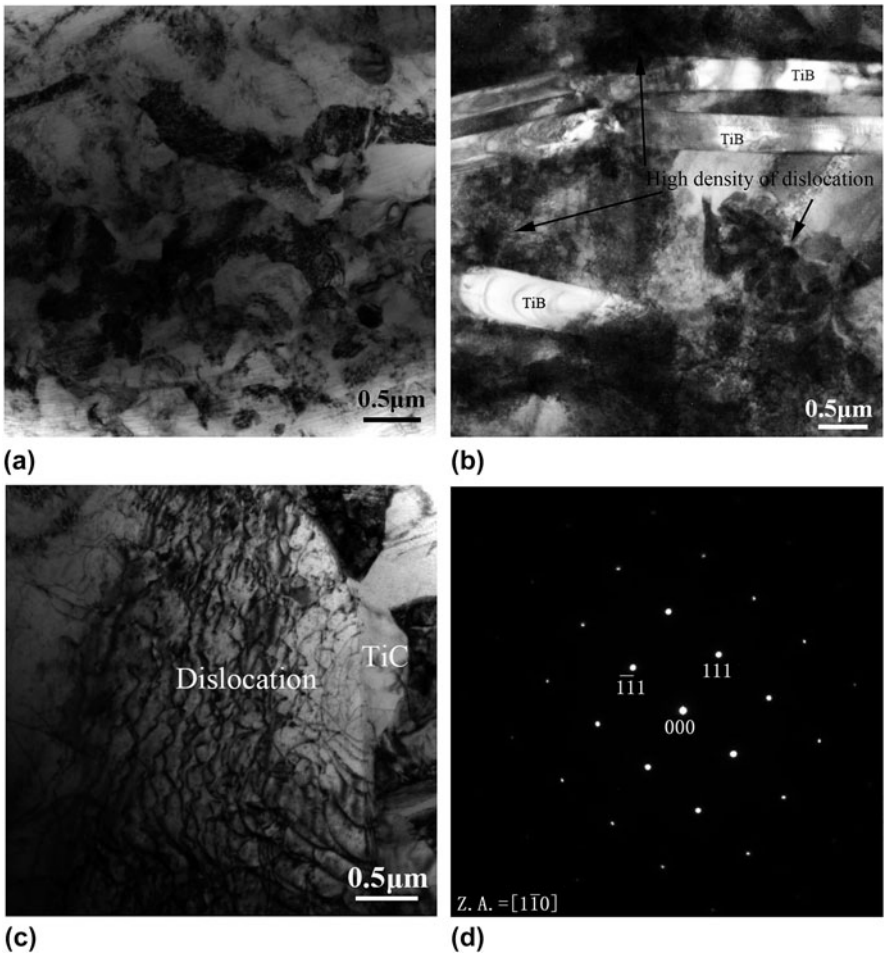



FIG. 4. TEM images showing microstructures of as-rolled composite sheet: (a) α subgrain, (b) near TiB whiskers, (c) near TiC particle, and (d) SAED pattern of TiC shown in (c).



https://doi.org/10.1557/jmr.2016.143 Published online by Cambridge University Press

dislocations and assist the nucleation of α phase, which contribute to the refinement of the substructures.

Figure 3 presents microstructure of the composite sheet after multistep rolling process at 1000 °C. As shown in Fig. 3(a), the morphology of TiC particles has no obvious differences under the rolling force compared to those within as-forged composites, while further fragmented TiB whiskers can be observed after rolling leading to decrease in average length and aspect ratio of the TiB whiskers, which are 9.1 μm and 4.2, respectively. Additionally, the distribution of both TiC particles and TiB whiskers are similar to Fig. 2(a) with a more obvious arrangement along the rolling direction. It can also be observed from Fig. 3(a) that the voids between the reinforcement ends and matrix existing in as-forged composites [Fig. 2(b)] can be completely closed after rolling due to the increase of matrix flow. The matrix microstructure of as-rolled TiB/Ti composite consists of equiaxed primary α and some residual transformed β phase can be seen at higher magnification SEM micrograph in Fig. 3(b), which is usually obtained after hot working in the lower (α + β) phase field. The primary α phase with an average thickness of about 7.46 μm and volume fraction of ~85% is elongated by rolling force and then chiefly arranges along the rolling direction. And the aspect ratio of the primary α measured to be 1.87 is reduced compared to that of as-forged composites, suggesting the occurrence of globularization after rolling.

The microstructure of the as-rolled composite sheet was investigated clearly in TEM samples, as shown in Fig. 4. As presented in Fig. 4(a), high density of dislocations and several subgrains are obviously observed in the primary α grains, indicating that dynamic recovery occurs in the microstructure during hot-rolling process. Additionally, the dislocation density near TiB whiskers and TiC particles shown in Figs. 4(b) and 4(c) is much higher than that within matrix shown in Fig. 4(a). The dislocations density of the composite is influenced by thermal expansion coefficients and plastic deformation coordination between the matrix and the particles. During the multistep rolling process, the dislocation density can be increased because of the different thermal expansion coefficients and the accumulative strain. Therefore, dislocations near the reinforcements are increased compared to those far from the reinforcements.

## B. Tensile properties

Figure 5 presents the room-temperature tensile stress–strain curves of the differently processed composites. The relative tensile properties are summarized in Table I. It can be seen from Fig. 5 and Table I, after TMP, significant enhancement in strength and elongation is obtained. For instance, compared to the as-cast composite, the tensile strengths of the as-forged and rolled composites are severally raised to about 12.5 and 24%, while the improvement in elongation is about 150 and 375%, respectively. The significant strengthening effect after TMP is primarily related to grain refinement strengthening and load-sharing effect of reinforcements. The grain refinement strengthening usually dominates the enhancement in tensile strength of the composites with low volume fraction of reinforcements.[16]

Based on the classic Hall–Petch mechanism, the yield strength (YS) can be improved by microstructural refinement. For titanium matrix with fully lamellar structures, the tensile properties are determined by the α colony size which impacts on the effective slip length of dislocations. And the slip length of dislocations can be further reduced with the precipitation of $\alpha_p$.[24] After TMP, fully lamellar structures of as-cast composites (Fig. 1) are broken down and transformed to the bimodal structure (Fig. 2) and then equiaxed structures (Fig. 3) accompanied by increase in the content of $\alpha_p$ and reduction in the size of $\alpha_p$. Therefore, the YS of the composite is gradually enhanced after forging and rolling. Meanwhile, the strengthening effect can be partly due to the high density of dislocations and substructures generated during TMP, as shown in Figs. 2(c) and 4(a). Moreover, the substructures in the as-rolled composite [Fig. 4(a)] are

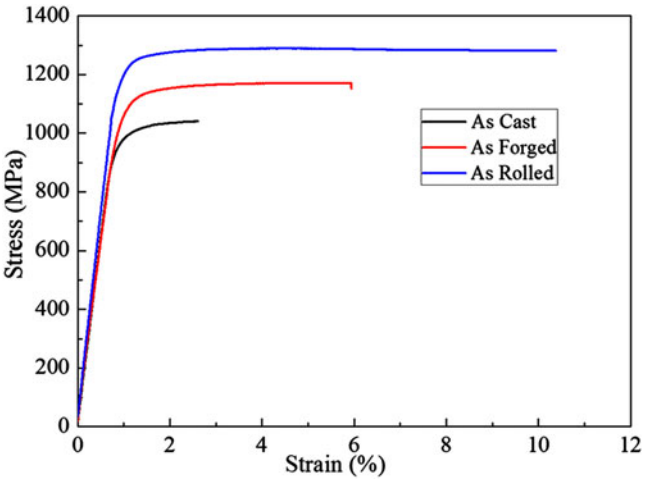



FIG. 5. Typical RT tensile stress–strain curves of the differently processed composites.

TABLE I. Average tensile properties of the differently processed composites at ambient temperature.

| | Room temperature | | |
|---|---|---|---|
| Processing state | UTS (MPa) | YS (MPa) | δ (%) |
| As cast | 1039.8 ± 14.3 | 975.5 ± 20.3 | 1.98 ± 0.39 |
| As forged | 1169.3 ± 7.3 | 1087.8 ± 18.7 | 4.95 ± 0.22 |
| As rolled | 1288.7 ± 5.1 | 1215.6 ± 14.9 | 9.4 ± 1.3 |

https://doi.org/10.1557/jmr.2016.143 Published online by Cambridge University Press

finer than those within the as-forged composite [Fig. 2(c)] due to the larger deformation, resulting in the higher strength of the as-rolled composite, as shown in Fig. 5 and Table I.

The other important factor contributing to enhance in strength is derived from load transfer at TiB and TiC. The micrographs of fracture surfaces for the differently processed composites presented in Fig. 6 reveal that most of

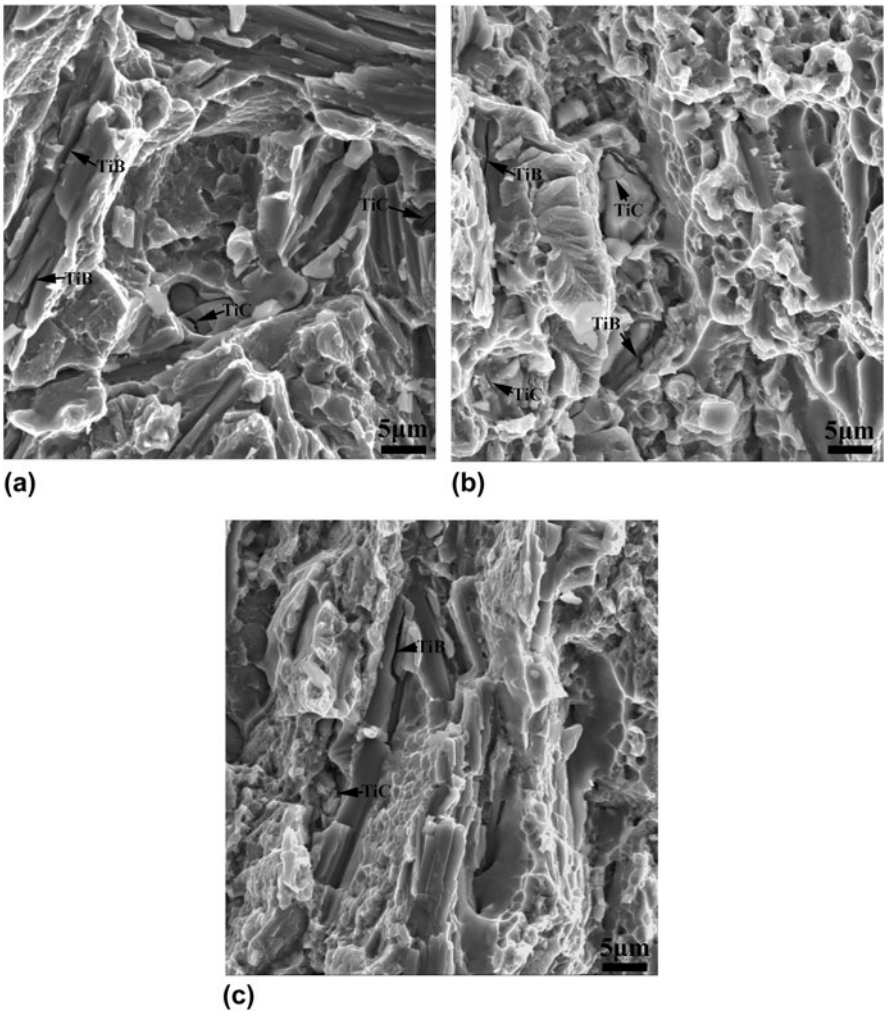



FIG. 6. Scanning electron micrographs of the fracture surfaces of the differently processed composites tensile-tested at RT: (a) as-cast, (b) as-forged, and (c) as-rolled.

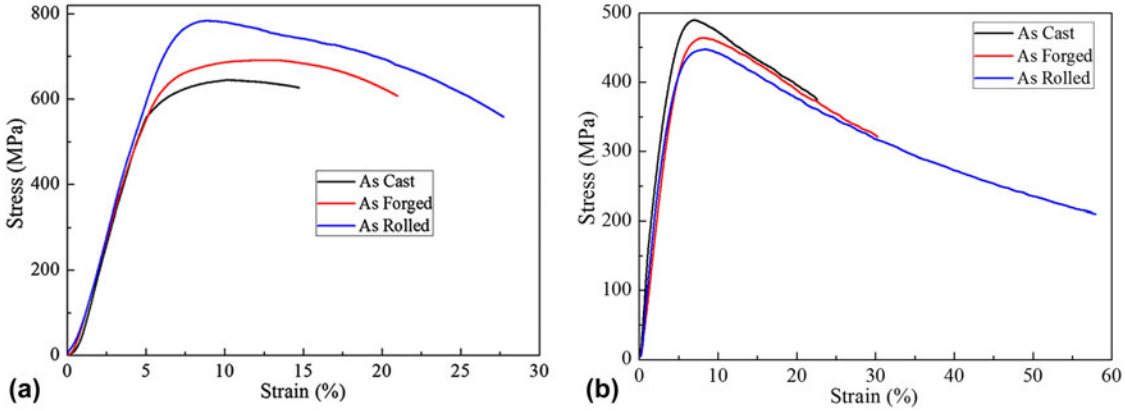



FIG. 7. Typical tensile stress–strain responses of the differently processed composites: (a) 600 °C and (b) 700 °C.



https://doi.org/10.1557/jmr.2016.143 Published online by Cambridge University Press

the TiB whiskers and TiC particles fracture during tensile test regardless of the processing states, indicating that the interfacial bonding strength is strong enough to transfer load from matrix to reinforcements. In addition, TMP improves the reinforcements' distribution of the composites, as shown in Figs. 2 and 3. Previous literature[11,25] demonstrated that the increase in distribution of reinforcements is beneficial to the tensile properties of particles reinforced TMCs. For the composites with even particle distribution, slip of dislocations can be resisted as an intense internal stress formed at the interface under the applied load, leading to increase in strength.[26]

TABLE II. Average tensile properties of the differently processed composites at elevated temperature.

| | 600 °C | | 700 °C | |
|---|---|---|---|---|
| Processing state | UTS (MPa) | δ (%) | UTS (MPa) | δ (%) |
| As cast | 646.5 ± 8.2 | 9.6 ± 1.5 | 488.3 ± 6.3 | 18.6 ± 2.8 |
| As forged | 691.2 ± 5.3 | 14.8 ± 3.2 | 462.6 ± 4.5 | 25.2 ± 3.4 |
| As rolled | 783.4 ± 2.9 | 21.7 ± 2.1 | 447.3 ± 1.6 | 55.8 ± 6.1 |

The enhancement of ductility after TMP can mainly be ascribed to the different matrix microstructure. As known crack sources are generated at reinforcements and then the crack propagates into titanium matrix simultaneously.[9] Guo[27] has pointed out that the fine equiaxed α can shorten the mean-free-path between the α phases, thereby hindering cavities to grow. After TMP, increase in the content of $\alpha_p$ and reduction in the size of $\alpha_p$ can be observed in Figs. 2 and 3. In consequence, the cavities meet with more barriers during the course of propagation, which leads to more tensile deformation and obtains high tensile ductility. In addition, the improvement of reinforcements' distribution after TMP can effectively avoid the premature failures in both reinforcement-free and reinforcement-rich areas, thereby contributing to the increase in ductility, as shown in Fig. 5 and Table I. The good ductility after TMP can be confirmed by the micrographs of fracture surfaces composites shown in Fig. 6. The fracture surface of the as-cast

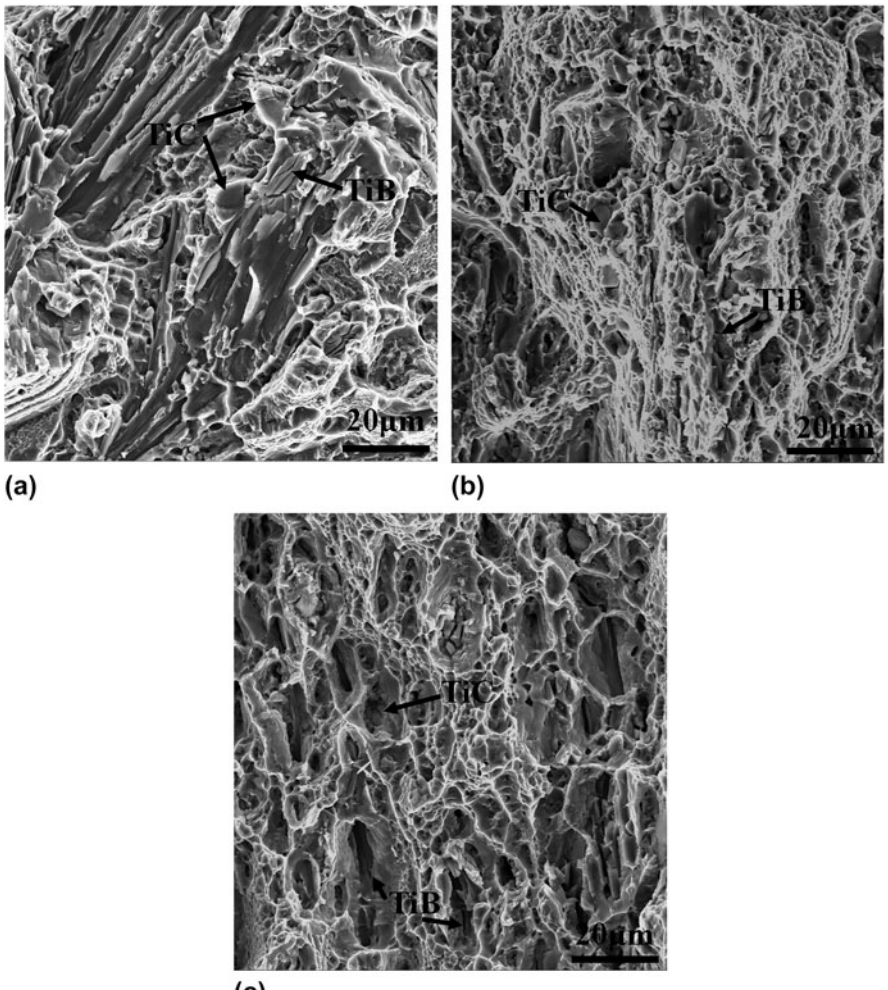



FIG. 8. Scanning electron micrographs of the fracture surfaces of the differently processed composites tensile-tested at 600 °C: (a) as-cast, (b) as-forged, and (c) as-rolled.

https://doi.org/10.1557/jmr.2016.143 Published online by Cambridge University Press

composite mainly consists of tear ridges and few dimples [Fig. 6(a)] while ductile dimples can be observed in the fracture surface of as-forged and as-rolled composites [Figs. 6(b)–6(c)].

The typical high-temperature tensile stress–strain curves and the relative tensile results of the differently processed composites are shown in Fig. 7 and Table II, respectively. It is obvious from Fig. 7 and Table II that, as compared to RT, lowering of ultimate tensile strength (UTS) and increase in elongation in all conditions for the composites are observed at high temperature. The degradation in UTS and increase in elongation at high temperature can be mainly ascribed to the matrix softening. Actually, the phenomenon is commonly found in the previous studies on TMCs.[28] After TMP, the UTSs of the composites improve significantly compared to that of the as-cast condition at 600 °C, exhibiting the similar changing trend with that at RT. Therefore, it is certain that strengthening factors including the improvement in distribution of reinforcements and the formation of dislocations, substructures, and grain refinement during TMP are still effective at 600 °C. Moreover, load transfer strengthening can be confirmed by fracture patterns of the composites shown in Fig. 8, i.e., that reinforcement fracture and no particle pull-out features can be observed in fracture surfaces of the composites with different processing states. The increasing dimples shown in Fig. 8 indicate the enhanced ductility [Fig. 7(a) and Table II] after TMP.

As tensile temperature increases to 700 °C, however, the UTSs of the composites gradually reduce while the elongations of the composites are enhanced remarkably after TMP, as shown in Fig. 7(b) and Table II. Obviously, current results indicate that TMP is of no help to improving UTS of the as-cast composite at 700 °C. Main reason is that the test temperature is 700 °C which is far higher than the equicohesive temperature of the matrix alloy.[29] So coarse grains can effectively hinder the grain boundary sliding while the microstructural refinement (Figs. 2 and 3) induced by TMP weakens UTS of the

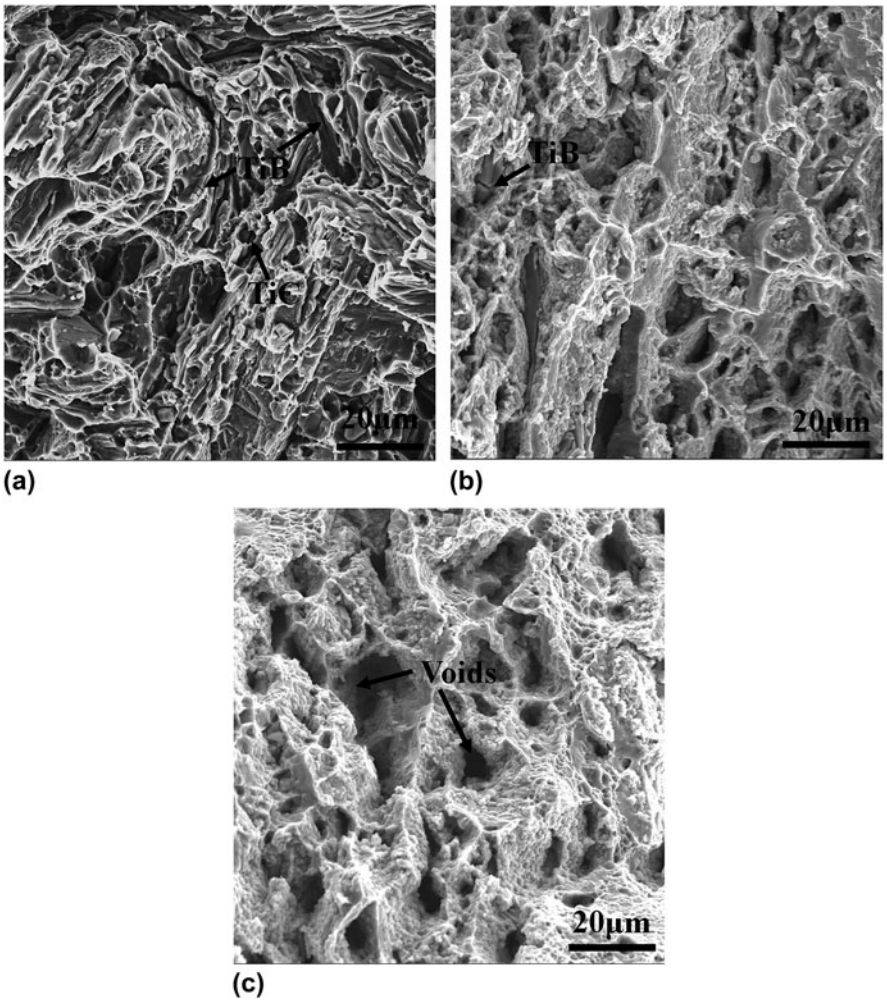



FIG. 9. Scanning electron micrographs of the fracture surfaces of the differently processed composites tensile-tested at 700 °C: (a) as-cast, (b) as-forged, and (c) as-rolled.



https://doi.org/10.1557/jmr.2016.143 Published online by Cambridge University Press

composites at 700 °C instead. In addition, the load transfer mechanism is based on the good interfacial adhesion. However, at 700 °C, dimples and few reinforcements pull-out can be observed in the fracture surfaces of composites shown in Fig. 9, especially the as-forged and rolled composites [Figs. 9(b)–9(c)], revealing a large amount of plastic deformation of matrix exceeds the reinforcements. Undoubtedly, the weak interfacial bonding at 700 °C make the load transfer mechanism ineffective. Therefore, the UTS of the composites gradually decrease after TMP as a joint result of the two factors mentioned above.

## IV. CONCLUSIONS

The following conclusions can be drawn from this study:

(1) TMP can significantly refine the microstructure of the as-cast composite. The matrix microstructure is transformed from fully lamellar microstructure to bimodal microstructure and then to equiaxed microstructure during forging and subsequent rolling. The distribution uniformity of reinforcements is greatly improved as well after TMP.

(2) Compared with the as-cast composite, TMP can significantly enhance the strength and elongation both at RT and 600 °C. The enhancement in strength is primarily ascribed to grain refinement, the formation of dislocations, and substructures as well as the improvement in distribution of reinforcements after TMP.

(3) At 700 °C, the UTSs of the composites gradually reduce while the elongations of the composites are enhanced remarkably after TMP. The degradation in UTS can be related to the matrix softening and interfacial debonding at 700 °C.

## ACKNOWLEDGMENTS

The authors gratefully thank the financial support from the National Natural Science Foundation of China (Nos. 51504163 and 51505323), The State Key Laboratory for Advanced Metal and Materials foundation (No. 2014-ZD06), the talent funded projects of Taiyuan University of technology (Nos. tyut-rc201342a and tyut-rc201343a) and the Special/Youth Foundation of Taiyuan University of Technology (No. 2013T001-T004).

## REFERENCES

1. S.C. Tjong and Y.W. Mai: Processing-structure-property aspects of particulate-and whisker-reinforced titanium matrix composites. *Compos. Sci. Technol.* **68**, 583 (2008).
2. K. Morsi, V.V. Patel, and K.S. Moon: Current activated pressure-assisted sintering (CAPAS) and nanoindentation mapping of dual matrix composites. *J. Mater. Sci.* **43**, 4050 (2008).
3. S. Gorsse and D.B. Miracle: Mechanical properties of Ti–6Al–4V/TiB composites with randomly oriented and aligned TiB reinforcements. *Acta Mater.* **51**, 2427 (2003).
4. D. Hill, R. Banerjee, and D. Huber: Formation of equiaxed alpha in TiB reinforced Ti alloy composites. *Scr. Mater.* **52**, 387 (2005).
5. O.M. Ivasishin, R.V. Teliovych, and V.G. Ivanchenko: Processing, microstructure, texture, and tensile properties of the Ti–6Al–4V–1.55B eutectic alloy. *Metall. Mater. Trans. A* **39**, 411 (2008).
6. L.J. Huang, L. Geng, and H.X. Peng: In situ ($TiB_w$ + $TiC_p$)/Ti6Al4V composites with a network reinforcement distribution. *Mater. Sci. Eng., A* **527**, 6726 (2010).
7. C.F. Yolton: The pre-alloyed powder metallurgy of Titanium with boron and carbon additions. *JOM* **56**, 56–59 (2004).
8. S.C. Tjong and Z.Y. Ma: Microstructural and mechanical characteristics of in situ metal matrix composites. *Mater. Sci. Eng., R* **29**, 67 (2000).
9. W.J. Lu, D. Zhang, and X.N. Zhang: Microstructure and tensile properties of in situ (TiB + TiC)/Ti6242 (TiB: TiC = 1:1) composites prepared by common casting technique. *Mater. Sci. Eng., A* **311**, 142 (2001).
10. V. Imayev, R. Gaisin, and E. Gaisina: Effect of hot forging on microstructure and tensile properties of Ti–TiB based composites produced by casting. *Mater. Sci. Eng., A* **609**, 39 (2014).
11. H.A. Rastegari, S. Asgari, and S.M. Abbasi: Producing Ti–6Al–4V/TiC composite with good ductility by vacuum induction melting furnace and hot rolling process. *Mater. Des.* **32**, 5010 (2011).
12. T. Wang, H.Z. Guo, and Y.W. Wang: Influence of processing parameters on microstructure and tensile properties of TG6 titanium alloy. *Mater. Sci. Eng., A* **528**, 736 (2010).
13. X. Li, S.Q. Lu, and M.W. Fu: The optimal determination of forging process parameters for Ti–6.5Al–3.5Mo–1.5Zr–0.3Si alloy with thick lamellar microstructure in two phase field based on P-map. *J. Mater. Process. Technol.* **210**, 37 (2010).
14. J.Q. Qi, H.W. Wang, and C.M. Zou: Influence of matrix characteristics on tensile properties of in situ synthesized TiC/TA15 composite. *Mater. Sci. Eng., A* **553**, 60 (2012).
15. C.J. Zhang, F.T. Kong, and S.L. Xiao: Evolution of microstructure and tensile properties of in situ titanium matrix composites with volume fraction of (TiB + TiC) reinforcements. *Mater. Sci. Eng., A* **548**, 152 (2012).
16. I. Sen, S. Tamirisakandala, and D.B. Miracle: Microstructural effects on the mechanical behavior of B-modified Ti–6Al–4V alloys. *Acta Mater.* **55**, 4988 (2007).
17. S. Tamirisakandala, R.B. Bhat, and J.S. Tiley: Grain refinement of cast titanium alloys via trace boron addition. *Scr. Mater.* **53**, 1424 (2005).
18. Z.Q. Chen, Y.G. Li, and D. Hu: Role of alloying elements in microstructures of beta titanium alloys with carbon additions. *Mater. Sci. Technol.* **19**, 1397 (2003).
19. P. Nandwana, J.Y. Hwang, M.Y. Koo, J. Tiley, S.H. Hong, and R. Banerjee: Formation of equiaxed alpha and titanium nitride precipitates in spark plasma sintered TiB/Ti–6Al–4V composites. *Mater. Lett.* **83**, 203 (2012).
20. L.G. Huang, F.T. Kong, and Y.Y. Chen: Microstructure and tensile properties of Ti–6Al–4V–0.1B alloys of direct rolling in the near β phase region. *Mater. Sci. Eng., A* **560**, 145 (2013).
21. R. Srinivasan, M.D. Bennett, and S. Tamirsakandala: Rolling of plates and sheets from as-cast Ti–6Al–4V–0.1B. *J. Mater. Eng. Perform.* **18**, 394 (2008).
22. F.C. Ma, W.J. Lu, and J.N. Qin: Effect of forging and heat treatment on the microstructure of in situ TiC/Ti–1100 composites. *J. Alloys Compd.* **428**, 336 (2007).
23. M.J. Bermingham, S.D. McDonald, and K. Nogita: Effects of boron on microstructure in cast titanium alloys. *Scr. Mater.* **59**, 539 (2008).
24. G. Lütjering: Influence of processing on microstructure and mechanical properties of (α + β) titanium alloys. *Mater. Sci. Eng., A* **243**, 38 (1998).

https://doi.org/10.1557/jmr.2016.143 Published online by Cambridge University Press

25. D.R. Ni, L. Geng, and J. Zhang: Effect of $B_4C$ particle size on microstructure of in situ titanium matrix composites prepared by reactive processing of Ti–$B_4C$ system. *Scr. Mater.* **55**, 429 (2006).
26. H.Z. Ye and X.Y. Liu: Review of recent studies in magnesium matrix composites. *J. Mater. Sci.* **39**, 6154 (2004).
27. P. Guo, Y.Q. Zhao, and W.D. Zeng: The effect of microstructure on the mechanical properties of TC4–DT titanium alloys. *Mater. Sci. Eng., A* **563**, 107 (2014).
28. Z.G. Zhang, J.N. Qin, and Z.W. Zhang: Microstructure effect on mechanical properties of in situ synthesized titanium matrix composites reinforced with TiB and $La_2O_3$. *Mater. Lett.* **64**, 361 (2010).
29. L. Xiao, W.J. Lü, and J.N. Qin: High-temperature tensile properties of in situ-synthesized titanium matrix composites with strong dependence on strain rates. *J. Mater. Res.* **23**, 3068 (2008).

https://doi.org/10.1557/jmr.2016.143 Published online by Cambridge University Press